

Synthesis of Co—N—C catalysts from a glucose hydrochar and their efficient hydrogenation of nitrobenzene

YANG Yu, BU Yu, LONG Xing-lin, ZHOU Zhi-kang, WANG Jing, CAI Jin-jun*

(School of Chemical Engineering, Xiangtan University, Xiangtan 411105, China)

Abstract: A low-cost, green catalyst for nitrobenzene (NB) hydrogenation is needed for aniline production. We report the preparation of highly-dispersed Co particles supported on N-doped carbons by the hydrothermal treatment of glucose, followed by the pyrolysis of a mixture of urea, glucose hydrochar and cobalt nitrate in one-pot. The effect of the pyrolysis temperature on the microstructure of the catalysts was studied. Results indicated that the activity for NB hydrogenation was highly affected by the surface area, Co-loading level and Co-N_x coordination in the catalysts. Co@NCG-800 pyrolyzed at 800 °C with 10% Co in the precursor had extraordinary activity for NB hydrogenation, achieving full conversion and 99% aniline selectivity in isopropanol at 100 °C and 1 MPa H₂ pressure for 2.5 h. NB conversion and aniline selectivity over the catalysts remained almost unchanged after six recycles, due to the strong coordination between the N- and Co-species. The reaction system showed not only a high NB activity but also a green and durable catalytic process, with easy operation, easy separation and catalyst reusability.

Key words: Biomass glucose; Hydrothermal; Co-N-C catalysts; Nitrobenzene hydrogenation

1 Introduction

Reduction or hydrogenation of nitrobenzene (NB) are 2 main strategies to produce anilines^[1-3] which is one of important intermediates for chemicals *i.e.* pesticide, dye and pigment. In particular, NB hydrogenation over these catalysts is a widely developed strategy, and almost 70% of anilines are produced by this method^[4]. For instance, sucrose-based Co—N—C catalysts had high activity in NB conversion using formic acid as a H₂ donor^[5], which can be magnetically recovered with high recyclability from the effect of uniformly N-species and Co particles on the surface. As compared to stoichiometric reduction with chemical H₂, hydrogenation using H₂ gas is eco-friendly and cost-effective for NB conversion into anilines^[6], in which a key issue is to find catalysts with high activity and selectivity under mild condition.

Heterogeneous catalysts using carbons as substrate have been reported for hydrogenation *i.e.* noble metals, non-noble metals and metal-free carbons, using H₂ as a reductant. Noble metals such as Pd, Pt or Ru as active centers have good catalytic perfor-

mances^[7-9]. Pd-loaded carbon tubes owned high activity with TOF value of 66 900 h⁻¹ and aniline selectivity of 99% for NB hydrogenation^[10]. Vanyorek et al.^[11] reported carbon black anchored Pd-Pt catalysts using NiO or Fe₂O₃ as promoter, showing little difference in activity and selectivity at a wide temperature range and 2 MPa H₂, while activation energy of catalysts was low of 7.6 kJ/mol. Pd, N-doped carbon foam also used in NB hydrogenation^[12], and NB conversion with 99.1% aniline yield and 99.8% selectivity reached regardless of temperature. Carbon tubes with P, N-species and B-N co-doped graphenes were also reported as the metal-free catalysts for nitroarene hydrogenation^[13-15], while the comparable activity was only observed as pressure over 3 MPa and reaction time up to 15 h.

As comparison, non-noble metal-based carbons *i.e.* M—N—C (M=Fe, Co or Ni) also had amazing activities and low costs,^[16] and great progress has achieved even if their activity is still slightly inferior to that noble metal-based carbons^[17-21]. Co—N—C catalysts as pyrolyzed by hybrids of melamine, Co(NO₃)₂ and polyacrylonitrile had good activity in nitroarene reduction^[22], and the catalyst with fluffy

Received date: 2022-11-30; Revised date: 2023-01-29

Corresponding author: CAI Jin-jun, Associated professor. E-mail: caijj@xtu.edu.cn

Author introduction: YANG Yu, Master student. E-mail: 2763129287@qq.com

mesopores and rich N-species showed both a full conversion and aniline selectivity at 120 °C and 1 MPa H₂. Recently, numerous methods have been reported to prepare M–N–C catalyst, especially for pyrolysis of zeolite imidazolate framework (ZIFs)^[23–25], because they often have advantages of high surface area, hierarchical pores, high N content from imidazole, and easily substitution of metals from different metal salts. For instance, Co–N co-doped carbons were derived by ZIF-67 pyrolysis and the size modulated by content of imidazole^[3], exhibiting a full conversion and aniline selectivity over 99% at 1 MPa H₂. NB hydrogenation did not occur after etching to remove Co-species^[3], indicating the synergistic effect between Co and N-species. Liu and co-workers reported the design of hollow CoS_x anchored on N-doped carbons by ZIF-67 pyrolysis and NH₃ etching^[26], and S-defect in catalysts was positive to achieve high activity for nitro compounds hydrogenation at 100 °C and 1.6 MPa H₂. It is admitted that N-species are useful to adjust electronic of carbon atom and uniformly stabilize ultrafine metals, boosting activity of M–N_x coordination. However, ZIFs production required long time and prohibitive cost in the linkers and pyrolysis also largely reduced yield, limiting their practical use in mass production. It is necessary to seek a green and scalable method to create Co–N–C catalysts for the better use of hydrogenation reaction.

Herein, we reported a facile method to incorporate Co-species into N-doped carbons through hydrothermal treatment of glucose biomass, followed by pyrolysis of hybrid of hydrochar, Co(NO₃)₂ and urea in one-pot. This route is low-cost and renewable using glucose as the carbon source and urea as N source,

where N-doped carbons with dispersed Co-species and Co–N_x sites easily achieved by urea decomposition as the form of gas during pyrolysis. The as-made Co–N–C catalysts were highly active and stable for NB hydrogenation. A full conversion of NB with a selectivity over 99% towards anilines was achieved. Besides, the present catalysts are more resistant to deactivation.

2 Experimental

2.1 Preparation of Co–N–C catalysts

The catalysts were obtained by one-pot pyrolysis of glucose hydrochar, Co(NO₃)₂ and urea. Hydrochar was formed by hydrothermal using ZnCl₂ as the catalyst to accelerate hydrolysis^[27–28], and a scheme was presented in Fig. 1. Firstly, 6 g of glucose and 18 g ZnCl₂ were dissolved in 60 mL water by sonication, and then sealed in autoclave to conduct hydrothermal reaction at 180 °C for 12 h. Precipitates were washed with water to clear impurities, followed by filtration and dried at 100 °C for 24 h. Then, 2 g of hydrochar as G-HTC, 4 g of urea, and 0.986 g of Co(NO₃)₂·6H₂O (of around 10% Co-species on G-HTC in mass) were mixed into powders, followed by the pyrolysis at 600–900 °C for 2 h under N₂ flow, ramping of 4 °C/min. As a result, samples were named as 10%Co@NCG-*T*, and *T* referred to temperature, for example 10%Co@NCG-800 indicated pyrolysis at 800 °C. To observe the effect of Co-species, loadings of Co-species also varied to be of 5% and 15%, and the samples were named as 5%Co@NCG-800 and 15%Co@NCG-800. As a control, NCG-800 in the absence of Co-species was obtained by similar procedure only without the presence of Co(NO₃)₂ in pyrolysis.



Fig. 1 Schematic diagram for the production of Co–N–C catalysts

2.2 Characterization

Morphology and structure of catalysts were studied by X-ray diffraction (XRD), scanning and transmission electron microscopy (SEM, TEM). Porosity was studied by N_2 isotherms and surface areas were collected by the Brunauer-Emmett-Teller (BET) method in p/p_0 range of 0.05-0.25. X-ray photoelectron spectroscopy (XPS) was used to study coordination, where C 1s peak at 284.8 eV was used as basis to calibrate binding energy. Apparatus information can be found elsewhere^[3,21].

2.3 Procedure for hydrogenation reaction.

Mixture of isopropanol (20 mL), catalysts (50 mg), and NB (150 mg) was added in a 50 mL autoclave, and air was removed by H_2 purging for 3 times. Reaction was performed at various H_2 pressures and temperatures with stirring at 500 r/min, and catalysts were collected by centrifugation. Liquid was studied on an Agilent 6890N gas chromatograph equipped with Agilent HP-1INNOW AX capillary column. The conversion and aniline selectivity were determined by internal standard of chlorobenzene based on integral areas of chromatographic peaks^[3], and all tests were replicated for 3 times. Moreover, the reusability of catalysts was done for 6 runs, which were washed by ethanol and thermally treated under N_2 flow at 800 °C for 1 h before the next cycle.

3 Results and discussion

3.1 Structural analysis

The morphology was observed by SEM observation, and all samples owned a well-defined spherical shape in diameter of about 5 μm with varying degree in breakage depending on pyrolysis conditions. G-HTC had mainly microspheres with identical sizes and smooth surface (Fig. 2a), which is a common characteristic for hydrochar using carbohydrates as sources^[29]. In general, glucose hydrochar had singly-dispersed spheres using water as media which was widely observed by different groups^[29-31], but these spheres for G-HTC were partially cross-linked from $ZnCl_2$ catalytic effect in hydrolysis. The existing $ZnCl_2$ was effective to increase particle size as com-

pared with hydrochar using pure H_2O as reaction media^[32]. However, Co-N-C catalysts had much rougher surface especially for these catalysts pyrolyzed at higher temperatures as shown in Fig. 2b-d, due to Co-assisting graphitization of amorphous carbons. The particle sizes of catalysts were largely shrinkaged caused by pyrolysis as compared to that of G-HTC, while doping Co-species did not affect shape, and samples still remained spheres with partial breakage regardless of pyrolysis conditions. Breakage for 10%Co@NCG was more obviously as an increase of temperature, and a lot of small particles were observed on surface. Other samples not shown here also had similar shape to that of 10%Co@NCG. A fluffy-like shape with numerous cavities was observed as temperature up to 900 °C (Fig. 2d). Hydrochar with Co-particles were ever obtained by one-pot hydrothermal of sucrose, $Co(NO_3)_2$ and melamine^[5], and further pyrolysis yielded Co-N-C catalyst in nanosheets, showing high-efficiency for the transfer hydrogenation of nitroarene with formic acid. The different procedures in the production of hydrochar would apparently affect the morphology of catalyst and also the catalysis performances.

The TEM images for 10%Co@NCG-800 confirmed the formation of Co particles with well-developed porosity (Fig. 3). Partial Co particles were singly-dispersed and wrapped by carbon layers with average thickness of ~ 28 nm, which is conducive to prevent Co-species from leaching during hydrogenation.

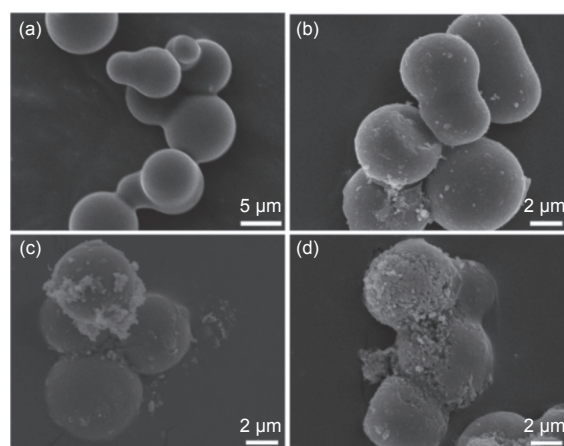


Fig. 2 SEM images for different catalysts: (a) G-HTC, (b) 10%Co@NCG-700, (c) 10%Co@NCG-800 and (d) 10%Co@NCG-900

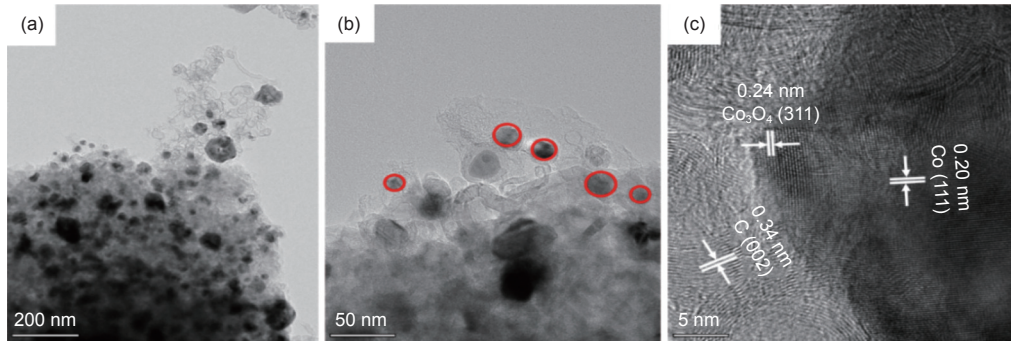


Fig. 3 Typical TEM images for 10%Co@NCG-800 under varied magnifications

tion. The results indicated that original Co^{2+} in oxidation were able to effectively reduce by self-reduction of carbons, being inclined to agglomerate and form large particles with irregular shape on carbon matrix. Some graphitic nanosheets were also formed by the catalytic effect of Co-species during pyrolysis. The high-resolution TEM images indicated the lattice structures with distance of 0.20 and 0.24 nm (Fig. 3c), owing to (111) plane of metallic Co and (311) plane of Co_3O_4 in oxidation^[2,21], respectively, and the distance of 0.34 nm was also observed for (002) plane of graphite.

The porosities were assessed by N_2 isotherms

with pore size distributions (PSD) (Fig. 4). As shown in Fig. 4a, NCG-800 obtained by co-pyrolysis of G-HTC and urea showed type IV isotherms with hysteresis loop in p/p_0 range of 0.45-0.95, indicating the presence of small-sized mesopores^[28]. The samples adsorbed N_2 at low pressure even with a limited amount, indicating the presence of partial micropores in the networks, probably formed by the decomposition of nitrides and volatiles in the form of small gas molecules (*e.g.* H_2O , NH_3 and CO_2) during pyrolysis^[29]. PSD curves determined by density functional theory (DFT) also supported the formation of hierarchical micro- and mesopores (Fig. 4b) and large

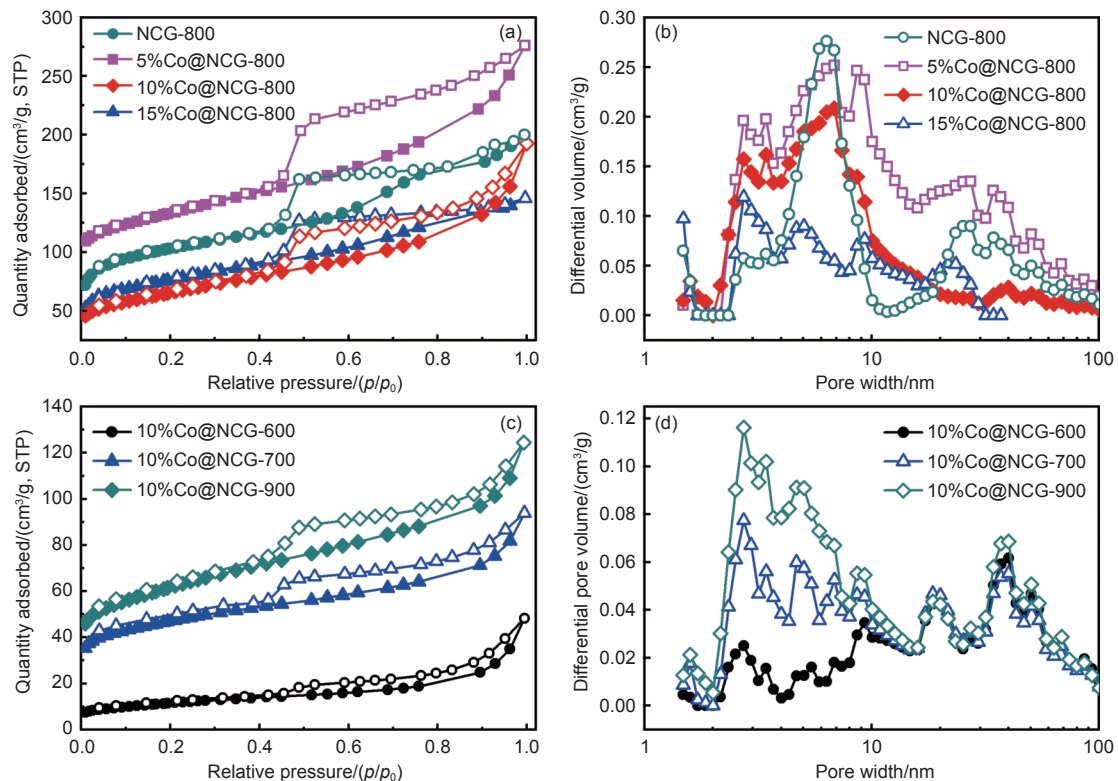


Fig. 4 (a, c) N_2 isotherms and (b, d) PSDs, and isotherms in Fig. 4a were separately shifted up by $30 \text{ cm}^3/\text{g}$ for shake of clarity

majority of pores located in a wide range. The calculated BET surface areas of NCG-800 were 204 m²/g, which is normal for carbons from hydrochar pyrolysis even if the existing urea can be also served as etching reagent^[32]. Isotherms for Co-N-C catalysts as pyrolyzed at 800 °C in Fig. 4a showed a similar situation to that of metal-free NCG-800, including an obvious hysteresis loop in p/p_0 range of 0.45-0.95. The adsorbed N₂ amounts still had a slightly increase as p/p_0 close to 1.0 especially for 5% and 10%Co@NCG-800, indicating the presence of wide PSD in mesopores or even partial macropores probably due to the shrinkage of pore wall under the assistance of Co-species^[33]. The PSDs results in Fig. 4b indicated that 5%Co@NCG-800 even possess large-sized mesopores in the 20-30 nm range. Besides, isotherms for Co-N-C catalysts as pyrolyzed at other temperatures also showed hysteresis loop (Fig. 4c), and the adsorbed amounts were highly enhanced as an increase of pyrolysis temperature, indicating the development of porosity from fully release of volatiles. As a result, the calculated surface areas for Co-N-C catalysts had an increase trend as temperature increased from 600 to 800 °C, while the further increase of pyrolysis temperature up to 900 °C caused a slightly decrease in the surface areas, probably due to shrinkage of carbon skeleton and wreckage of pores by excessive pyrolysis. BET surface areas of 10%Co@NCG catalysts were of 42, 170, 273 and 196 m²/g, corresponding to the pyrolysis at 600, 700, 800 and 900 °C, respectively. The increase of Co-loadings slightly reduced porosity from partially porous blockage, and surface areas for 5% and 15%Co@NCG-800 were of 294 and 227 m²/g, respectively. Pore volumes for catalysts also had a similar trend, and total pore volumes for 5% and 15%Co@NCG-800 were of 0.35 and 0.30 cm³/g, respectively. The detailed pore parameters were presented in Table 1, and average pores for 5%, 10%, and 15%Co@NCG-800 were of 4.75, 3.30 and 5.23 nm, respectively. As compared to that NCG-800, the larger surface areas in Co-N-C pyrolyzed at same temperature were caused by a possible reaction of cobalt oxides with carbon matrix and decomposition of

cobalt salts with more volatiles release to yield pores^[25]. Admittedly, a high ratio of pores in the range of 2-10 nm associating with large surface areas were beneficial for substrates diffusion and adsorption, exposing more active sites for liquid-phase hydrogenation.

To evaluate the variation of crystal structures, XRD patterns were shown in Fig. 5. Admittedly, all catalysts owned a broad peak at around 21° from (002) plane for amorphous carbons^[19]. Intensity of (002) peak slightly lowered for the series of 10%Co@NCG pyrolyzed at different temperatures as compared to that of metal-free NCG-800. Co-N-C catalysts also had evident shoulder peaks at 44.2°, 51.5° and 75.8° from (111), (200) and (220) plane of Co particles^[22], respectively, indicating partial formation of metallic Co from a self-reduction effect of carbons. Besides, a weak peak at 36.8° was observed for Co-N-C catalyst from (311) plane for Co₃O₄, confirming that the self-reduction was not enough to re-

Table 1 Porous parameters for these catalysts obtained from different conditions

Catalysts	^[a] S _{BET} (m ² /g)	^[b] V _t (cm ³ /g)	^[c] V _{meso} (cm ³ /g)	^[d] D _{ave} (nm)
NCG-800	204	0.16	0.13	3.19
10%Co@NCG-600	42	0.08	0.07	7.24
10%Co@NCG-700	170	0.14	0.11	3.42
10%Co@NCG-800	273	0.23	0.16	3.30
10%Co@NCG-900	196	0.19	0.14	3.92
5%Co@NCG-800	294	0.35	0.26	4.75
15%Co@NCG-800	227	0.30	0.24	5.23

Note: ^[a] Surface areas;

^[b] Total pore volumes;

^[c] Mesopore volumes for pores larger than 1.7 nm;

^[d] Average pore sizes determined by 4 V/A method.

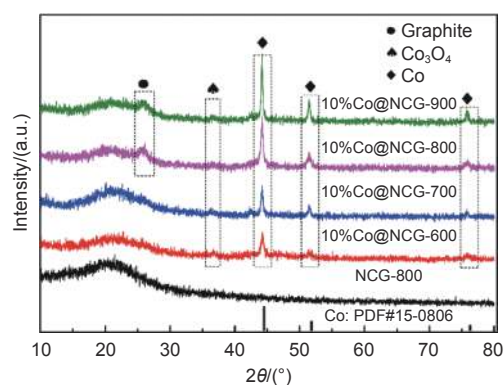


Fig. 5 XRD patterns for the series of catalysts

duce all Co in oxidation into metallic particles and partially crystal oxides still existed. As shown in Fig. 5, intensity of peaks from Co-species was highly enhanced as an increase of pyrolysis temperature, while half-width of peaks did not change into narrower mode, indicating that high-temperature was positive to self-reduction for the formation of metallic Co particles from oxides. That is to say, due to strong reduction of carbon materials, the relative content of metal Co particles in the frameworks increases as the increase of pyrolysis temperature, and particle sizes do not increase obviously. Significantly, 10%Co@NCG catalysts even contained a peak at 25.6° from crystal plane of graphite as temperature up to 800°C ^[2], owing to the catalytic effect of Co-species. It should be admitted that the XRD patterns for 5% and 15%Co@NCG-800 not shown here also showed similar peaks to that of 10%Co@NCG-800 only with change in intensity, due to the different content of Co-loadings in precursor. As a result, 10%Co@NCG-800 catalysts with well-developed mesopores, large surface areas, and high contents of

metallic Co particles would probably exhibit the highest activity in NB hydrogenation.

3.2 Elemental analysis

XPS measurements for 10%Co@NCG-800 were performed to evaluate its compositions. As shown in Fig. 6a, the main peaks at around 285.1, 400.2, 532.1 and 780.1 eV were observed for energy values of C1s, N1s, O1s and Co2p, respectively^[2,4], indicating the successfully doping of Co- and N-species on the surface of carbons by one-pot pyrolysis. Admittedly, peak intensity for N1s is relative weak, and urea as nitrogen source is probably not ideal for doping during the pyrolysis, and the content of C, N, O, and Co-species in composition of 10%Co@NCG-800 was 91.4 at.%, 0.5 at.%, 6.1 at.% and 2.0 at.%, respectively. High-resolution of C1s spectra in Fig. 6b were fitted into 4 peaks at 284.7, 285.6, 286.6 and 290.5 eV, due to the bonding of C=C, C=N, C-N/C-O and C=O, respectively^[31]. The presence of C-N and C=N peaks indicates successful N-doping *via* one-pot pyrolysis. The deconvolution of N1s spectra in Fig. 6c showed 3 peaks centering at about 398.6, 399.9 and

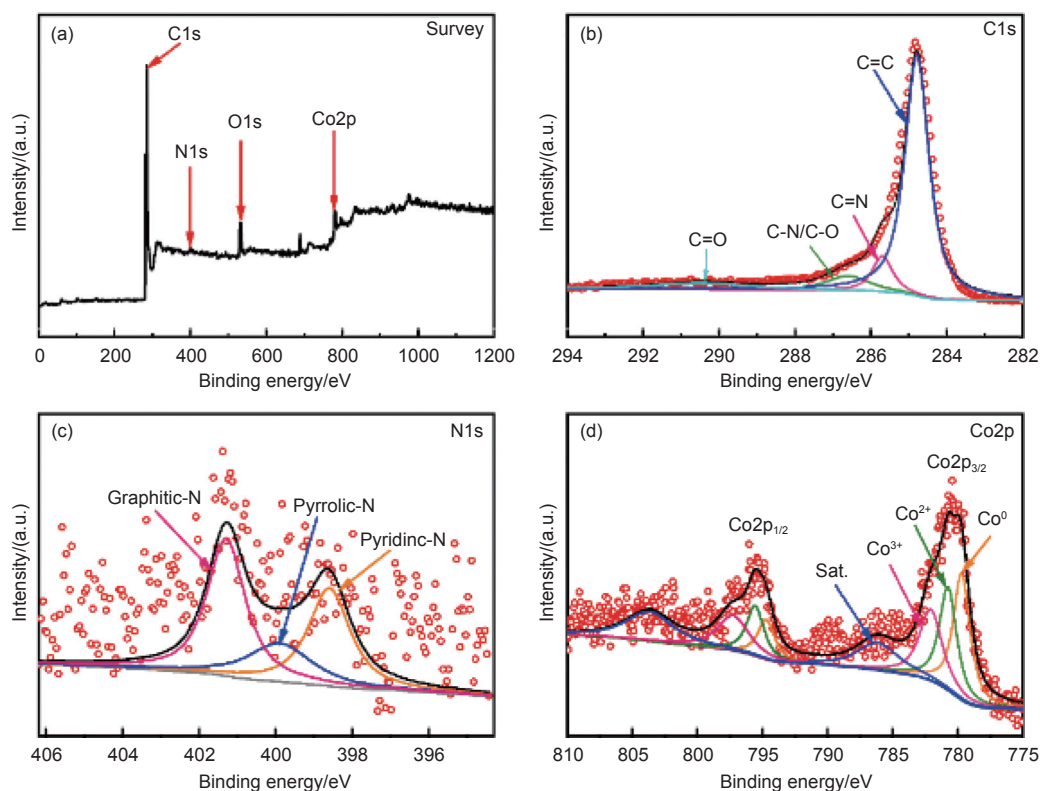


Fig. 6 XPS spectra of 10%Co@NCG-800: (a) survey curve, and high resolution XPS: (b) C1s, (c) N1s and (d) Co2p

401.2 eV, owing to pyridinic, pyrrolic and graphitic-N, respectively^[3,5]. The peak intensity of pyrrolic N was the lowest due to partially thermal conversion into other N-species, and the intensity for graphitic-N was much higher than that of pyridinic N from catalytic effect of Co particles at high-temperature pyrolysis conditions^[19]. As a result, the calculated relative ratio for graphitic, pyridinic and pyrrolic N was separately 44.62%, 34.49% and 20.88% in total N-species on the surface of 10%Co@NCG-800. The pyridinic N often located at edges or defects of carbon layer and provided an electron pair, which was conducive to the attachment of metal particles, resulting in a positive effect towards the formation of Co-N_x sites. High-resolution of Co2p XPS spectra in Fig. 6d includes 2 main peaks at 780.3 and 795.4 eV for Co2p_{1/2} and Co2p_{3/2}^[21], where the binding energies for Co2p_{3/2} peak were fitted into signals of Co(0) (779.7 eV), Co²⁺ (780.7 eV) and Co³⁺ (782.1 eV), and intense signal in Co(0) peak confirmed crystallinity of Co particles from CoO_x due to self-reduction effect of carbon layers^[33]. Two signals at 786.2 and 803.7 eV were satellite peaks for Co2p_{3/2} and Co2p_{1/2}. All these results indicate the successfully encapsulating of Co and N-species into carbons to form Co–N–C catalysts with the co-existence of Co-N_x and Co-O_x sites, which was believed to facilitate H₂ dissociation in following hydrogenation reaction.

3.3 Catalytic performance

The transformation of NB into anilines was used as a model reaction to evaluate the catalytic performance of Co–N–C catalysts. As shown in Table 2, no aniline was observed in the product when no catalyst used or glucose hydrochar used as catalyst, indicating that catalysts were imperative in reaction. Using NCG-800 as catalyst, the NB conversion was of only 11% with aniline selectivity up to 100% because aniline was the only product from NB hydrogenation. It was noted that the presence of N-species in carbon catalysts was positive for catalytic performance despite a limited activity from single N-dopant under mild conditions, which was confirmed by others using heteroatoms-doped carbon nanotubes as metal-

free catalysts for NB hydrogenation reaction^[13–15]. For instance, no activity was observed for N-doped carbon nanotubes as H₂ pressure lower than 2 MPa at 170 °C in early work^[13], and NB conversion was only of 60% with aniline selectivity up to 91% even as H₂ pressure up to 4 MPa for 10 h. Co–N–C catalysts with an equal content of cobalt salt as pyrolyzed at different temperatures had largely enhanced activity as compared to that G-HTC and NCG-800 without Co-species as summarized in Table 2, indicating that the presence of Co-species were critical for NB hydrogenation. As the pyrolysis temperature ranging from 600 to 800 °C, the catalytic activity over catalysts was proportional to temperature, and 10%Co@NCG-800 as pyrolyzed at 800 °C did show the best activity with a full NB conversion. Admittedly, the surface areas of catalysts were not decisive factor for catalytic activity, considering that 10%Co@NCG-600 as pyrolyzed at 600 °C with surface areas of only 42 m²/g also showed NB conversion of 86%. As the temperature increased up to 900 °C, 10%Co@NCG-900 reversely exhibited a lower NB conversion of 93.7% under the same conditions, resulting from the fact that catalysts with more highly graphitic sp² carbon structure were rather chemically inert to H₂ and therefore not benefited for NB hydrogenation^[34–35].

To understand Co-loadings on catalytic activity, the comparative results for catalysts pyrolyzed at 800 °C were studied. As shown in Fig. 7a, all catalysts with different Co-loadings can completely transform NB into aniline at 120 °C under conditions of 1 MPa H₂ and reaction time up to 2.5 h. As temperature reduced to be 100 °C, both 10%Co@NCG-800 and 15%Co@NCG-800 still had a full NB conversion,

Table 2 NB hydrogenation over catalysts under conditions of 120 °C and 1 MPa H₂ with reaction time up to 3 h

Entry	Catalysts	Conversion (%)	Selectivity(%)
0	Blank	0	0
1	G-HTC	0	0
2	NCG-800	11.0	>99
3	10%Co@NCG-600	86.0	>99
4	10%Co@NCG-700	95.4	>99
5	10%Co@NCG-800	100	>99
6	10%Co@NCG-900	93.7	>99

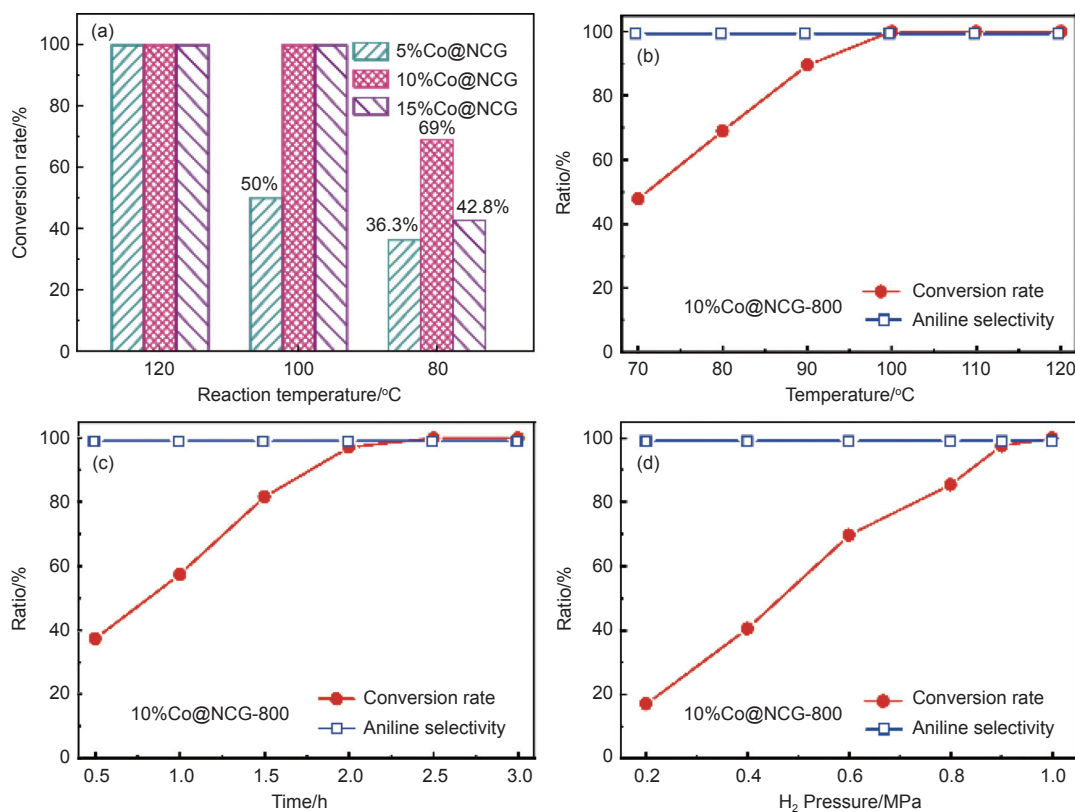


Fig. 7 (a) NB conversion on catalysts as pyrolyzed at 800 °C, and the effects of different reaction parameters on activity over 10%Co@NCG-800 catalyst: (b) temperature, (c) time and (d) H₂ pressure

while the NB conversion for 5%Co@NCG-800 was only of 50%. Significantly, the NB conversion for 10%Co@NCG-800 still remained 69% as reaction temperature decreased to 80 °C, much higher than that of other two catalysts under the same condition (Fig. 7a), and 10%Co@NCG-800 featured in hierarchical micro-mesopores also promoted transportation of substrates, intermediates and products^[16]. All the results indicates that a higher temperature was effective for hydrogenation, and the presence of moderate Co-species in catalyst was important for catalytic process under mild conditions. Combined with TEM results (Fig. 3), agglomeration of Co particles caused by excessive doping may be the main reason for the reduction of catalytic activity over 15%Co@NCG-800. The effects of reaction conditions such as temperature, time, and H₂ pressure on NB hydrogenation over 10%Co@NCG-800 as an example were also assessed to determine optimum conditions. The aniline selectivity changed a little with value close to be 100% regardless of reaction conditions, while the

higher reaction temperature, longer reaction time associating with the higher H₂ pressure largely affected catalytic activity. As shown in Fig. 7b, the conversion rate of NB largely increased as the increase of reaction temperature, where the conversion was around 50% at 70 °C and then increased to be a full conversion at 100 °C, and further increase of temperature unchanged the conversion rate. Similarly, the reaction time and initial H₂ pressure also showed positive effect towards activity (Fig. 7c, d), where NB were fully transformed into anilines as reaction time up to 2.5 h and H₂ pressure up to 1 MPa. For instance, NB conversion was enhanced from 37% to 98% as time extended from 0.5 to 2.0 h under conditions of 100 °C and 1 MPa H₂ pressure (Fig. 7c), and a full conversion was achieved as reaction time up to 2.5 h. All the phenomena confirmed the superiority of 10%Co@NCG-800 for NB hydrogenation under mild conditions of 100 °C, 2.5 h, and 1 MPa H₂ pressure, constituting to be one of the best conditions for NB hydrogenation from the viewpoint of sustainable

chemistry. For instance, full conversion was ever observed on Co–N–C catalysts at higher pressure or longer reaction time as reaction temperature lower than 120 °C^[3,17], separately from the pyrolysis of ZIF-67 and ZIF-9 particles. As for the mechanism, the adsorbed H₂ molecules on Co–N–C catalyst were dissociated into 2 hydrogens, and the yielded H-species reacted with nitro group to form nitroso compounds. Then, nitroso group combined with H-species to yield phenylhydroxylamine, followed by the reduction from the adsorbed H₂ to form aniline^[3], and desorbed into solution. During the process, 10%Co@NCG-800 with hierarchical micro-mesopores benefited for transportation of substrates, intermediates, and aniline products.

3.4 Reusability

The catalytic activity of Co–N–C catalysts for NB hydrogenation in successive runs was explored under the optimal condition of 100 °C, 1 MPa H₂ pressure, and reaction time up to 1 h. The results of using 10%Co@NCG-800 as an example were compiled in Fig. 8. The catalysts were treated by ethanol, calcined again at 800 °C, and then continued to be used for hydrogenation. As shown in Fig. 8a, aniline yield was close to 50.3% and catalysts can be recycled up to 6 cycles with activity fluctuation in a small range, overcoming the commonly deactivation for hydrogenation in liquid-solution. The aniline yield

after 5 recycles was still highly up to 49%. Admittedly, the catalysts after the first cycle without calcination had a big loss in the activity, which is similar to our previous work using MOFs as precursors to obtain Co–N–C catalysts^[3], owing to the formation of cobalt oxides from metallic Co species during recycle reactions. After simple calcination, the catalysts showed good activity and stability for NB hydrogenation. It is not difficult to understand that the ratio of cobalt oxides in the system would be reduced and metallic Co-species enhanced by self-reduction of carbon materials during the calcination process in inert atmosphere. XRD patterns for catalysts after 6 recycles were measured (Fig. 8b) and no newly formed peaks were observed. The intensity for diffraction peaks from metallic Co was reduced for the used catalysts, confirming the occurrence of partial interactions between active metal particles and substrate during the reaction^[33]. All the above-mentioned results indicate that the distinctive activity of Co–N–C catalyst mainly originates from synergistic effects between metallic Co and Co-N_x coordination, not cobalt in oxidation state in carbon substrates.

4 Conclusion

N-doped carbons incorporating Co particles were obtained by one-pot pyrolysis using glucose hydrochar and urea as precursors, acting as high-efficient catalysts for NB hydrogenation. The effects of Co-loadings and pyrolysis temperature on catalytic activity were studied, and 10%Co@NCG-800 had the best performance with a full NB conversion and aniline selectivity over 99% at conditions of 100 °C and 1 MPa H₂ up to 2.5 h. The catalyst had good reusability even after 6 times reuse under the best condition with aniline yield remaining to be of over 50%. The formation of Co-N_x coordination inhibited agglomeration of metal particles, and coating of metallic Co in carbon layers effectively reduced the leaching of active site, resulting in the excellent activity and stability. The present approach opened-up a facile method to produce other earth-abundant metal catalysts for NB conversion.

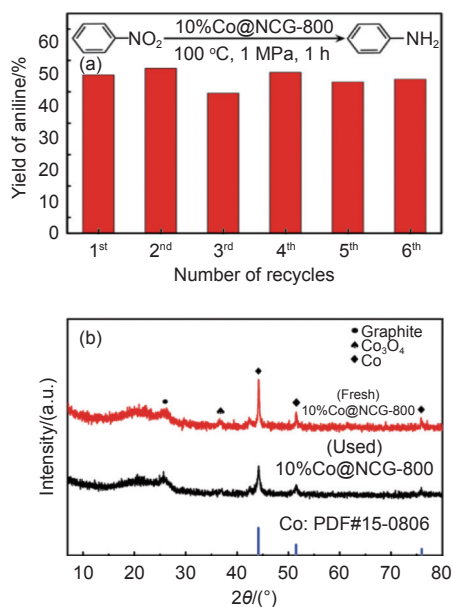


Fig. 8 (a) The reusability of 10%Co@NCG-800 and (b) XRD patterns for the fresh and used catalysts

Declaration of competing interest

There is no competing interest or personal relationships to influence the work reported in this paper.

Date availability statement

The data that support the findings of this study are openly available in Science Data Bank at <https://www.doi.org/10.57760/sciencedb.j00125.00009> or <https://resolve.pid21.cn/31253.11.sciencedb.j00125.00009>.

Acknowledgements

National Natural Science Foundation of China (21506184), Education Bureau of Hunan Province (21B0098), Project of Guiding Technology of Xiangtan City (CG-ZDJH202120) and Undergraduate Innovation and Entrepreneurship Training Project of Xiangtan University.

References

- [1] Qiao C, Jia W, Zhong Q, et al. MOF-derived Cu-nanoparticle embedded in porous carbon for the efficient hydrogenation of nitroaromatic compounds[J]. *Catalysis Letters*, 2020, 150(12): 3394-3401.
- [2] Xu Y, Shan W, Liang X, et al. Cobalt nano-particles encapsulated in nitrogen-doped carbon shells: Efficient and stable catalyst for nitrobenzene reduction[J]. *Industrial & Engineering Chemistry Research*, 2020, 59(10): 4367-4376.
- [3] Wang D, Wei J, Wang J, et al. MOFs carbonization: In-situ encapsulation of Co-species into N-doped carbons as highly efficient catalysts for nitrobenzene hydrogenation[J]. *Diamond and Related Materials*, 2022, 121: 108748.
- [4] Song T, Ren P, Duan Y, et al. Cobalt nano composites on N-doped hierarchical porous carbon for highly selective formation of anilines and imines from nitroarenes[J]. *Green Chemistry*, 2018, 20(20): 4629-4637.
- [5] Yuan M, Long Y, Yang J, et al. Biomass sucrose-derived cobalt@nitrogen-doped carbon for catalytic transfer hydrogenation of nitroarenes with formic acid[J]. *ChemSusChem*, 2018, 11(23): 4156-4165.
- [6] Sun X, Olivos-Suarez A I, Osadchii D, et al. Single cobalt sites in mesoporous N-doped carbon matrix for selective catalytic hydrogenation of nitroarenes[J]. *Journal of Catalysis*, 2018, 357: 20-28.
- [7] Nandi D, Siwal S, Choudhary M, et al. Carbon nitride supported palladium nanoparticles: An active system for the reduction of aromatic nitro-compounds[J]. *Applied Catalysis A: General*, 2016, 523: 31-38.
- [8] Leng F, Gerber I C, Lecante P, et al. Controlled and chemoselective hydrogenation of nitrobenzene over Ru@C60 catalysts. *ACS Catalysis*, 2016, 6 (9): 6018-6024.
- [9] Goyal V, Sarki N, Poddar M K, et al. Biorenewable carbon-supported Ru catalyst for N-alkylation of amines with alcohols and selective hydrogenation of nitroarenes[J]. *New Journal of Chemistry*, 2021, 45(32): 14687-14694.
- [10] Sun Z, Zhao Y, Xie Y, et al. The solvent-free selective hydrogenation of nitrobenzene to aniline: An unexpected catalytic activity of ultrafine Pt nanoparticles deposited on carbon nanotubes[J]. *Green Chemistry*, 2010, 12(6): 1007-1011.
- [11] Prekob Á, Muránszky G, Szöri M, et al. Preparation of highly effective carbon black supported Pd–Pt bimetallic catalysts for nitrobenzene hydrogenation[J]. *Nanotechnology*, 2021, 32(42): 425701.
- [12] Prekob Á, Szamosvölgyi Á, Muránszky G, et al. Palladium decorated N-doped carbon foam as a highly active and selective catalyst for nitrobenzene hydrogenation[J]. *International Journal of Molecular Sciences*, 2022, 23(12): 6423.
- [13] Xiong W, Wang Z, He S, et al. Nitrogen-doped carbon nanotubes as a highly active metal-free catalyst for nitrobenzene hydrogenation[J]. *Applied Catalysis B: Environmental*, 2020, 260: 118105.
- [14] Chen X, Shen Q, Li Z, et al. Metal-free H₂ activation for highly selective hydrogenation of nitroaromatics using phosphorus-doped carbon nanotubes[J]. *ACS Applied Materials & Interfaces*, 2020, 12(1): 654-666.
- [15] Yang F, Cao Y, Chen Z, et al. Large-scale preparation of B/N co-doped graphene-like carbon as an efficient metal-free catalyst for the reduction of nitroarenes[J]. *New Journal of Chemistry*, 2018, 42(4): 2718-2725.
- [16] Michalke J, Haas M, Krisch D, et al. Generation of cobalt-containing nanoparticles on carbon via pyrolysis of a cobalt corrole and its application in the hydrogenation of nitroarenes[J]. *Catalysts*, 2022, 12(1): 11.
- [17] Hu A, Lu X, Cai D, et al. Selective hydrogenation of nitroarenes over MOF-derived Co@CN catalysts at mild conditions[J]. *Molecular Catalysis*, 2019, 472: 27-36.
- [18] Lyu D, Mollamahale Y B, Huang S, et al. Ultra-high surface area graphitic Fe-N-C nanospheres with single-atom iron sites as highly efficient non-precious metal bifunctional catalysts towards oxygen redox reactions[J]. *Journal of Catalysis*, 2018, 368: 279-290.
- [19] Li Y, Zhang X, Ren J, et al. Hierarchical porous nitrogen-doped carbon material with Fe-NX as an excellent electrocatalyst for oxygen reduction reaction[J]. *Catalysis Communications*, 2022, 165: 106439.
- [20] Chen L, Liu X, Zheng L, et al. Insights into the role of active site density in the fuel cell performance of Co-N-C catalysts[J]. *Applied Catalysis B: Environmental*, 2019, 256: 117849.
- [21] Wang D, Luo M, Yue L, et al. Co-embedded N-doped hierarchical porous biocarbons: Facile synthesis and used as highly efficient catalysts for levulinic acid hydrogenation[J]. *Fuel*, 2022, 329: 125364.
- [22] Cui X, Liang K, Tian M, et al. Cobalt nanoparticles supported on N-doped mesoporous carbon as a highly efficient catalyst for the synthesis of aromatic amines[J]. *Journal of Colloid and Interface Science*, 2017, 501: 231-240.
- [23] Wang J, Wang Y, Hu H, et al. From metal–organic frameworks to

- porous carbon materials: recent progress and prospects from energy and environmental perspectives[J]. *Nanoscale*, 2020, 12(7): 4238-4268.
- [24] Gao C, Mu S, Yan R, et al. Recent advances in ZIF-derived atomic metal –N –C electrocatalysts for oxygen reduction reaction: Synthetic strategies, active centers, and stabilities[J]. *Small*, 2022, 18(14): 2105409.
- [25] Yang S, Peng L, Oveisi E, et al. MOF-derived cobalt phosphide/carbon nanocubes for selective hydrogenation of nitroarenes to anilines[J]. *Chemistry-A European Journal*, 2018, 24(17): 4234-4238.
- [26] Zhang G, Tang F, Wang L, et al. ZIF-67 derived CoS_x/NC catalysts for selective reduction of nitro compounds[J]. *Journal of Central South University*, 2021, 28(5): 1279-1290.
- [27] Liang Y, Huang G, Zhang Q, et al. Hierarchical porous carbons from biowaste: Hydrothermal carbonization and high-performance for Rhodamine B adsorptive removal[J]. *Journal of Molecular Liquids*, 2021, 330: 115580.
- [28] Huang G, Wang Y, Zhang T, et al. High-performance hierarchical N-doped porous carbons from hydrothermally carbonized bamboo shoot shells for symmetric supercapacitors[J]. *Journal of the Taiwan Institute of Chemical Engineers*, 2019, 96: 672-680.
- [29] Hou Z, Tao Y, Bai T, et al. Efficient Rhodamine B removal by N-doped hierarchical carbons obtained from KOH activation and urea oxidation of glucose hydrochar[J]. *Journal of Environmental Chemical Engineering*, 2021, 9(4): 105757.
- [30] Zhang Z, Luo D, Hui G, et al. In-situ ion-activated carbon nanospheres with tunable ultramicroporosity for superior CO₂ capture[J]. *Carbon*, 2019, 143: 531-541.
- [31] Feng J, Cai R, Magliocca E, et al. Iron, nitrogen Co-doped carbon spheres as low cost, scalable electrocatalysts for the oxygen reduction reaction[J]. *Advanced Functional Materials*, 2021, 31(46): 2102974.
- [32] Xu L, Guo L, Hu G, et al. Nitrogen-doped porous carbon spheres derived from d-glucose as highly-efficient CO₂ sorbents[J]. *RSC Advances*, 2015, 5(48): 37964-37969.
- [33] Ma X, Zhou Y X, Liu H, et al. A MOF-derived Co-CoO@N-doped porous carbon for efficient tandem catalysis: dehydrogenation of ammonia borane and hydrogenation of nitro compounds[J]. *Chemical Communications*, 2016, 52(49): 7719-7722.
- [34] Zhang G, Tang F, Wang X, et al. , Atomically dispersed Co–S–N active sites anchored on hierarchically porous carbon for efficient catalytic hydrogenation of nitro compounds[J]. *ACS Catalysis*, 2022, 12(10): 5786-5794.
- [35] Zhang L, Shang N, Gao S, et al. Atomically dispersed Co catalyst for efficient hydrode-oxygenation of lignin-derived species and hydrogenation of nitroaromatics[J]. *ACS Catalysis*, 2020, 10(15): 8672-8682.

葡萄糖基水热炭构建 Co–N–C 催化剂及其硝基苯催化加氢反应性能

杨 雨, 卜 钰, 龙兴霖, 周志康, 王 静, 蔡进军*

(湘潭大学 化工学院, 湖南 湘潭 411105)

摘 要: 硝基苯选择性加氢反应是生产苯胺的重要方法, 其关键在于开发一种具有高效选择性且低成本的绿色催化剂。本文基于葡萄糖水热炭化得到水热炭前驱体, 结合尿素和硝酸钴一步高温热解制备了一种高度分散的富含 Co 纳米颗粒的氮掺杂多孔炭材料, 将其作为催化剂用于硝基苯加氢反应。详细研究了热解温度对催化剂结构和催化活性的影响, 证实了催化活性主要受催化剂的比表面积、Co 掺杂量及其 Co-N_x 配位效应的影响。结果表明, 将含 10%Co 源制备的前驱体 800 °C 热解得到的催化剂 (Co@NCG-800) 表现出优异的硝基苯催化加氢性能, 在以异丙醇为溶剂、100 °C 和 1 MPa 氢压下反应 2.5 h 时可实现硝基苯的转化, 苯胺选择性高达 99%。催化剂循环使用 6 次后的硝基苯转化率和苯胺选择性几乎保持不变。优异的循环稳定性能可归因于多孔炭材料中的氮元素和 Co 纳米颗粒的强相互作用, 同时磁性 Co 纳米颗粒使得催化剂具有较好的分离特性和重复使用性。

关键词: 生物质葡萄糖; 水热炭化; Co-N-C 催化剂; 硝基苯加氢

中图分类号: X712 **文献标识码:** A

基金项目: 国家自然科学基金 (21506184); 湖南省教育厅优秀青年项目 (21B0098); 湘潭市科技计划指导项目 (CG-ZDJH202120); 湘潭大学大学生创新训练计划。

通讯作者: 蔡进军, 副教授. E-mail: caijj@xtu.edu.cn

作者简介: 杨 雨, 硕士研究生. E-mail: 2763129287@qq.com

本文的电子版全文由 Elsevier 出版社在 ScienceDirect 上出版 (<https://www.sciencedirect.com/journal/new-carbon-materials/>)